

Papers published in *Hydrology and Earth System Sciences Discussions* are under open-access review for the journal *Hydrology and Earth System Sciences*

Filter properties of seam material from paved urban soils

T. Nehls¹, G. Jozefaciuk², Z. Sokolowska², M. Hajnos², and G. Wessolek¹

¹Institute of Ecology, Dept. of Soil Science, Technical University Berlin, Salzufer 11-12, 10587 Berlin, Germany

²Institute of Agrophysics of Polish Academy of Sciences, Doswiadczalna 4, 20-290 Lublin, Poland

Received: 9 August 2007 – Accepted: 13 August 2007 – Published: 15 August 2007

Correspondence to: T. Nehls (thomas.nehls@tu-berlin.de)

HESSD

4, 2625–2657, 2007

Filter properties of pavement seam materials

T. Nehls et al.

Title Page

Abstract

Introduction

Conclusions

References

Tables

Figures

◀

▶

◀

▶

Back

Close

Full Screen / Esc

Printer-friendly Version

Interactive Discussion

EGU

Abstract

We studied pavement seam material. This is the soil substrate in joints of pervious pavements in urban areas. It is mostly 1 cm thick and develops from the original seam filling by depositions of all kinds of urban residues, including anthropogenic organic substances. It was investigated, how this unique form of organic matter influences the filter properties of seam material and how the seam material influences heavy metal transport through the pavement. The seam material is characterised by a darker munsell colour, higher organic carbon content, higher surface areas, higher cation exchange capacities, but a lower fraction of high adsorption energy sites compared to the original seam filling. The deposited anthropogenic organic matter itself could be characterised as particulate and non-polar. Compared to natural soils, it has a small surface area and a low surface charge density resulting in a small cation exchange capacity of only 75 cmol(+) kg⁻¹C. The seam material shows stronger sorption of Pb and Cd compared to the original construction sand. The retardation capacity of seam material towards Pb is similar, towards Cd it is much smaller compared to natural soils. The simulated long term displacement scenarios for a street in Berlin do not indicate an acute contamination risk for Pb. For Cd the infiltration from ponds can lead to a displacement of Cd during only one decade.

1 Introduction

In urban areas, sealing of soil surfaces leads to ecological problems caused by the increased and accelerated runoff and reduced evapotranspiration compared to non-sealed soils (Fig. 1). Cities are normally drier and hotter than the surrounding areas. At heavy rainfalls the exceeding water causes mixed sewage systems to run over. This is one of the main threats to water quality of urban water bodies (Heinzmann, 1998). Therefore, run off reduction by increasing infiltration is among the main ideas of ecological urban planning. This goal can be reached by increased use of pervious

HESSD

4, 2625–2657, 2007

Filter properties of pavement seam materials

T. Nehls et al.

Title Page

Abstract

Introduction

Conclusions

References

Tables

Figures

◀

▶

◀

▶

Back

Close

Full Screen / Esc

Printer-friendly Version

Interactive Discussion

EGU

pavements. In many European cities, especially in the older parts, they are regularly found. They keep the convenience for the city dwellers but allow infiltration rates of 58 cm d^{-1} for a mosaic tile pavement with 20 % of seams, until 155 cm d^{-1} for so called grass pavers having an amount of open seams of up to 41% (Wessolek and Facklam, 1997).

The seams allow infiltration and the pavers reduce evaporation. Therefore, groundwater recharge rates are 99 to 208 mm a^{-1} in sealed areas compared to only 80 mm a^{-1} for a pine-oak forest around Berlin (Wessolek and Renger, 1998). If rain water accumulates in ponds on the pavements, the groundwater recharge can be greater than 300 mm a^{-1} . Ponds with up to 60 mm depth are no exception in old quarters. We gauged a pond in front of our department ($52^{\circ}31'4.03'' \text{ N}$; $13^{\circ}19'25.79'' \text{ E}$) with a volume of 56 L at a horizontal projection of only 2 m^2 . Rainwater runoff in urban areas is often contaminated, e.g. by heavy metals. Dannecker et al. (1990) and Boller (1997) found Pb concentrations of up to 0.3 mg L^{-1} in the street runoff, while Cd concentrations reached up to 0.0076 mg L^{-1} (Dierkes and Geiger, 1999). The high infiltration rates together with even low contaminant concentrations may result in severe contaminant fluxes (Dannecker et al., 1990). An assessment of the risk of soil and groundwater contamination requires hydraulic and sorption parameters for the according materials, which are the pavers and the construction material, mainly sand. Furthermore, after a while, a new horizon, the “seam material”, develops. The term “seam material” describes the soil material in between single pavestones of pavements, which developed from technogenic sand. It shows a very dark colour, is mostly only 1 cm thick and contains all kinds of deposited urban dirt like foliage, hairs, oil, dog faeces, food residues, cigarette stubs, glas – in short: any kind of urban waste, small enough to fit into the pavement seams, at least after being milled by pedestrians or cars. Thereby, pedestrians and cars abrase their soles and tires and these abrasions also end up in the seams. Furthermore seams contain great amounts of urban dust and therefore soot, concrete abrasions, aerosols and so on. While the hydraulical characteristics of the seam material have already been investigated (Nehls et al., 2006), the chemical

Filter properties of pavement seam materials

T. Nehls et al.

Title Page

Abstract

Introduction

Conclusions

References

Tables

Figures

◀

▶

◀

▶

Back

Close

Full Screen / Esc

Printer-friendly Version

Interactive Discussion

filter properties are still unknown. They can not be extrapolated from other soils because the organic carbon (C_{org}) of this material differs from non-urban, natural soils in origin, quality and function. For instance, the amount of black carbon, a “combustion-produced black particulate carbon, having a graphitic microstructure” (Novakov, 1984) is increased compared to non-urban soils (Nehls et al., 2007¹).

It is hypothesized, that because of its increased C_{org} contents, seam material acts as a valuable filter and influences transport processes through the pavement seams. Therefore, the motivation of this study was to assess the seam materials retardation potential for heavy metals under consideration of its special forms of organic matter, its source or sink function and its thickness. Therefore, (i) general surface and filter properties of the seam material were investigated in relation to C_{org} by ion exchange and water vapor adsorption measurements. Cation exchange capacity, surface area, surface charge density, and adsorption energy were studied. Thereby, the organic matter itself could be characterized. Furthermore (ii) the specific adsorption of Pb and Cd to the seam material and the according contamination status were studied. Thus, two relevant toxic heavy metals of different mobility and affinity to organic matter, were exemplarily studied. Finally, (iii) the heavy metal solute transport through the pavement system considering the seam material have been simulated using the investigated parameters.

2 Material and methods

Sites and sampling

Samples were taken in Berlin and Warsaw, two cities with similar climatic, geologic and geomorphologic conditions, but different industrial activity, traffic intensity and contamination history. The sampling sites were located close to roads or directly on roads.

¹Nehls, T., Brodowski, S., Amelung, W., and Zech, W.: Black Carbon in Paved Urban Soils, in preparation, 2007.

Filter properties of pavement seam materials

T. Nehls et al.

Title Page

Abstract

Introduction

Conclusions

References

Tables

Figures

◀

▶

◀

▶

Back

Close

Full Screen / Esc

Printer-friendly Version

Interactive Discussion

Filter properties of pavement seam materials

T. Nehls et al.

Title Page

Abstract

Introduction

Conclusions

References

Tables

Figures

◀

▶

◀

▶

Back

Close

Full Screen / Esc

Printer-friendly Version

Interactive Discussion

Samples consisted of the material that fills spaces between single stones of pavements. The dark seam material at 0 to 1 cm depth was always easily distinguishable from a much brighter 1 to 5 cm layer (Fig. 2). The upper layer is influenced by all external factors and deposits, while the deeper one was taken as representative of the original seam filling material, which is not severely altered by external deposits. The seam material was scraped up using one-way polyethylene teaspoons under suspicious observation of pedestrians.

In Berlin (B - samples), we sampled both the seam material and the original seam filling layer, while only the upper layer was sampled in Warsaw (W – samples). Samples were taken in the following streets: Monbijouplatz (B1, B1a), Weidendamm (B2, B2a), Schnellerstrasse (B3, B3a), from different places at the Grosser Stern (B4–B8, B4a), Emilii Plater (W1), Jerozolimskie (W2), Pulawska (W3), Rzymowskiego (W4), Stanow Zjednoczonych (W5), Modlinska (W6), Slowackiego (W7), Wilanowska (W8) and Rowecki Bridge (W9). Sampling sites were located on sidewalks within 2 m from roads with different traffic intensity, while samples from the Pfluegerstrasse (B9, B10) were sampled directly on the road. Samples B1a - B4a come from the same sites as B1–B4, the index “a” indicates that samples consist of original seam filling material (1 to 5 cm).

General chemical properties

The $\text{pH}(\text{CaCl}_2)$ and electric conductivity (EC) have been measured using standard methods (DIN-ISO 10390, DIN-ISO 11265). Munsell's color was determined for fresh samples. The potential cation exchange capacity (CEC_{pot}) was determined at pH 8.2 using a batch method with cation exchange and re-exchange (Mehlich, 1984) because of high EC of the samples. The total carbon content, C_{tot} and C_{org} (C_{org} after HCl-treatment to remove carbonates) were determined conductometrically after combustion (Carlo Erba, C/N analyzer).

Surface properties

Valuable substrate specific surface parameters can be obtained from very simple measurements, not requiring expensive equipment. The specific surface area (A_s) and the adsorption energies (E_a) were calculated from water vapor adsorption isotherms using the vacuum chamber method at the temperature $T=294\pm 0.1$ K. Prior to the adsorption measurement, soil sample aliquots of 3 g were dried in a hermetic chamber with concentrated sulphuric acid until constancy of weights. Then, they were exposed to 20 stepwise rising water vapor pressures (p/p_s) ranging from 0.005 to 0.98 which were controlled by sulfuric acid solutions. The samples were equilibrated with the corresponding water vapour until constancy of weights. The higher p/p_s is, the longer the time gets for equilibration, at the highest step more than one week was necessary. The amount of adsorbed water, a , was the difference between the weight of the humid sample and the dry sample (dried for 24 h at 378 K). Results of triple weightings had a coefficient of variation (CV) of 3.7%, averaged values were used for further calculations.

Aranovich's theory of polymolecular adsorption has been used to obtain the capacity of a mono-molecular layer from the experimental water vapour adsorption isotherms (Fig. 3). In contrast to the standard Brunauer-Emmett-Teller (BET) model (Brunauer et al., 1938), Aranovich's isotherm allows vacancies in the adsorbed layer and describes the polymolecular adsorption over a broader and more realistic range of p/p_s ($\approx 0.05 < p/p_s < 0.8$) than the BET does ($\approx 0.05 < p/p_s < 0.3$) (Aranovich, 1992):

$$a = \frac{a_m C p/p_s}{(1 + C p/p_s) \sqrt{(1 - p/p_s)}}, \quad (1)$$

where p/p_s [hPa hPa⁻¹] is the water vapour pressure, a [g] is the adsorbed amount of water at a given p/p_s , a_m [g] is the statistical monolayer capacity and $C = e^{\frac{E_a - E_c}{RT}}$, a constant related to the adsorption energy, E_a [J] and condensation energy of water, E_c

HESSD

4, 2625–2657, 2007

Filter properties of pavement seam materials

T. Nehls et al.

Title Page

Abstract

Introduction

Conclusions

References

Tables

Figures

◀

▶

◀

▶

Back

Close

Full Screen / Esc

Printer-friendly Version

Interactive Discussion

EGU

[J].
 Aranovich's isotherm was fitted to the experimental data (measured a vs. adjusted ρ/ρ_s) to derive values for a_m and C .

Having a_m , we calculated A_s [m²] of the sample using the following equation:

$$A_s = \frac{a_m L \omega}{M} \quad (2)$$

Here, L is the Avogadro number (6.02×10^{23} molecules per mole), M [g mol⁻¹] is the molecular mass of the adsorbate and ω is the area occupied by a single adsorbate molecule (1.08×10^{-19} m² for water). Knowing A_s , the surface charge density SCD [cmol(+) m⁻²] can be calculated:

$$SCD = \frac{CEC_{pot}}{A_s} \quad (3)$$

The adsorption energy distribution functions showing fractions f of surface sites of different adsorption energies, ($f(E_i)$), were calculated from adsorption isotherms data, using the theory of adsorption on heterogeneous surfaces (Jaroniec and Brauer, 1986). Aranovich's isotherm (Aranovich, 1992) was applied to describe local adsorption effects.

$$\Theta_\tau(p) = \frac{1}{\sqrt{1-x}} \sum_{i=1}^n \frac{C_i x}{(1 - C_i x) f(E_i)} \quad (4)$$

Here, C_i is the value of the constant C for sites of kind i . Solving Eq. (4) for $f(E_i)$ is an ill-conditioned problem. Small variation in experimental data caused by heterogeneity of the samples and detections capabilities of the balance leads to large variation in estimation of site fractions. Therefore, a condensation approximation CA was inserted (Harris (1968)). This method is based on the replacement of the local isotherm by a step-function. The final formula for the calculation of site fractions then becomes:

$$f(E_i) = \frac{\sqrt{1-x_{i+1}} \Theta_\tau(E_{i+1}) - \sqrt{1-x_i} \Theta_\tau(E_i)}{E_{i+1} - E_i} \quad (5)$$

Filter properties of pavement seam materials

T. Nehls et al.

Title Page

Abstract

Introduction

Conclusions

References

Tables

Figures

◀

▶

◀

▶

Back

Close

Full Screen / Esc

Printer-friendly Version

Interactive Discussion

From $f(E_i)$ values, the average water vapor adsorption energy, \bar{E}_a , can be calculated by the following equation as described by Jozefaciuk and Shin (1996):

$$\bar{E}_a = E_i f(E_i). \quad (6)$$

The calculation of adsorption energy distribution functions ($f(E_i)$ against E_i dependencies) was performed using Eq. (5). Energy values were expressed in the units of thermal energy (RT), as scaled energies ($\frac{E_a - E_c}{RT}$). A scaled energy equal to 0 represents an adsorption energy equal to the condensation energy of the vapor. The maximum adsorption energy in the condensation approximation is related to the minimum value of p/p_s which was around 0.004 in our case. This corresponds to an energy adsorption of around -5.5 . Thus, it was reasonable to assume -6 as the maximum energy for the samples. However, this value can be considered only as a first estimate of the maximum energy because of the lack of experimental data at small relative pressures. We arbitrarily set the maximum energy to -8 assuming that if there were no sites with higher adsorption energies than -6 , the corresponding values of $f(E_i)$ will be close or equal to zero. In order to reduce the noise of the measurements, only pairs of values, which differ for at least 2 units were used.

Adsorption isotherms for Cd and Pb

Adsorption isotherms were obtained for C_{org} affected, immobile Pb and mobile Cd according to OECD guideline 106 (OECD, 2000). One gram of soil has been equilibrated with 45 ml 0.01 M $CaCl_2$ overnight. Then, heavy metals were added as a typical cocktail (Pb, Cd, Ni, Cu, Zn) in 5 ml 0.01 M $CaCl_2$ solution for 48 h of equilibration. Thus, the resulting isotherms include realistic adsorption concurrence. For all samples five stepwise rising solute concentrations including distilled water were added. Therefore, the resulting adsorption isotherms include one desorption step and span over a wide range of concentrations (liquid concentrations range from 0.05 to 10 mg L^{-1} for Pb and from 0.001 to 5 mg L^{-1} for Cd). After two hours of shaking, the original pH of

Filter properties of pavement seam materials

T. Nehls et al.

Title Page

Abstract

Introduction

Conclusions

References

Tables

Figures

◀

▶

◀

▶

Back

Close

Full Screen / Esc

Printer-friendly Version

Interactive Discussion

Filter properties of pavement seam materials

T. Nehls et al.

Title Page

Abstract

Introduction

Conclusions

References

Tables

Figures

◀

▶

◀

▶

Back

Close

Full Screen / Esc

Printer-friendly Version

Interactive Discussion

the samples were re-adjusted with KOH. Liquid phase HM concentrations were measured in the supernatant after 20 min of centrifugation at $1000 \times g$. The according solid phase concentration was analyzed like following. In order to consider only the HM fraction which is involved in adsorption processes, the 0.025 M $(\text{NH}_4)_2\text{EDTA}$ (pH 4.6) extractable portion has been determined (Welp and Brummer, 1999) in advance for the individual samples. The difference of HNO_3 and EDTA extract is the residual amount which has not been considered as adsorbed phase. The samples were extracted with concentrated HNO_3 (soil/acid ratio = 1/20) for 360 min at 453 K under pressure. The concentrations of Pb and Cd were measured with a maximum CV of 2% and 5%, respectively.

For the fitting of an adsorption isotherm to the experimental data with complex solid phases like soils, the use of the Freundlich model is widely recommended (Stumm and Morgan, 1996) before Langmuir, because it does not expect similar energy sites but can be seen as a sum function of Langmuir isotherms for the individual energy sites (Sposito, 1980). So it is adequate to describe the seam material which is a mixture of sorbents with varying surface characteristics:

$$C_s = K_f C_l^m, \quad (7)$$

where C_s [mg kg^{-1}] is the sorbed concentration in the solid phase, C_l [mg L^{-1}] is the concentration in the liquid phase, K_f [$\text{mg}^{1-m} \text{L}^m \text{kg}^{-1}$] is the Freundlich distribution coefficient, describing the soil material's affinity to the solute. The exponent m is a measure for the linearity of the adsorption.

The adsorption characteristics are studied to describe the mobility of the heavy metals. A good method to compare different adsorption characteristics with different degrees of linearity is to calculate the retardation factor R , which derives from the convection-dispersion equation and describes the retardation of substances compared to a conservative, non sorbing tracer:

$$R = 1 + \frac{\rho_B}{\Theta} \frac{\partial C_s}{\partial C_l}, \quad (8)$$

where ρ_B [kg L⁻¹] is the dry bulk density and Θ [m³ m⁻³] is the water content of the soil. For non-linear adsorption of solutes R becomes:

$$R = 1 + \frac{\rho_B}{\Theta} m K_f C_l^{m-1} \quad (9)$$

Simulation of the Cd and Pb displacement

- 5 The filter effect of the seam material has been assessed by a numerical HM displacement simulation using the software HYDRUS 1D v2.02 (U.S. Salinity Laboratory USDA-ARS, 1991, Riverside, CA, USA). It solves Richard's equation numerically and applies the convection dispersion equation for the solute transport. It can work with Freundlich's adsorption model as well as with other concepts (Simunek et al., 1999).
- 10 The employed input data are shown in Table 1.

It was the goal to assess the impact of the chemical properties (special form of organic matter), the importance (thickness) and the source/sink function (contamination status) of the seam material on heavy metal displacement. The travel times were simulated through a 20 cm long column of (i) construction sand, (ii) a 1 cm thick seam material and 19 cm of construction sand and (iii) 20 cm of seam material. The soil hydraulic parameters of the site B9 have been applied while the chemical features of the sites B1, B2, B4 and B9 have been used for the simulation. Travel time in that context indicates the period of time which is required to recover 95% of the upper boundary concentration at the lower boundary of the column. The measured background concentrations in the soil were (a) ignored (no contamination) and (b) considered as initial conditions. So, six scenarios *ia*, *ib*, *iiia*, *iiib*, *iiia*, *iiib* have been simulated. Scenarios *ia* and *iiia* compare the maximum retardation capacity of the original construction material with that of the seam material, while in *iiia* the maximum retardation of the realistic soil material mixture is assessed. The scenarios *a* and *b* are then used to assess the actual source/sink potential of the construction sand and the seam material.

20

25

Groundwater recharge rates of 120 mm a⁻¹ (Wessolek and Renger, 1998) and of 480 mm a⁻¹ (simulating infiltration from ponds) were applied. Furthermore, the open

Filter properties of pavement seam materials

T. Nehls et al.

Title Page

Abstract

Introduction

Conclusions

References

Tables

Figures

◀

▶

◀

▶

Back

Close

Full Screen / Esc

Printer-friendly Version

Interactive Discussion

Filter properties of pavement seam materials

T. Nehls et al.

Title Page

Abstract

Introduction

Conclusions

References

Tables

Figures

◀

▶

◀

▶

Back

Close

Full Screen / Esc

Printer-friendly Version

Interactive Discussion

seam area of 27 %, measured at site B9, was included to get the daily groundwater recharge rates of 0.12 and 0.48 cm d⁻¹ for the open seam area as the net infiltration rate at the upper boundary. Thus, annual evapotranspiration has been indirectly considered, but seasonal variations have been disregarded. The water flow was not simulated but realized by accordingly chosen boundary conditions and derived effective parameters for the site B9: K_s^* of 0.12 and 0.48 cm d⁻¹, respectively and pressure heads of 0 cm for the upper and lower boundary conditions. The according artificial saturated water contents, Θ_s^* corresponded to K_s^* and was derived from $K(\Psi)$ and $\Theta(\Psi)$ functions fitted to measured porosity (Nehls et al., 2006) and K_s data (Table 1). For these measurements, 100 cm³ cylinders were filled with seam material up to bulk densities which have been determined using small cylinders which fitted in the intersection of seams on a cobble stone paved street (Fig. 4) (Nehls et al., 2006). For the original construction sand, undisturbed cylinders were taken from the layer beneath the pavestones.

For simulating the contaminated material, measured liquid equilibrium concentrations were applied (see Table 1) which were in the range of the measured adsorption isotherms.

The rain water runoff concentrations at the upper boundary for Pb and Cd were chosen to be 0.3 and 0.01 mg L⁻¹, respectively. The solute transport balance for the simulations always had an relative error of less than 5%. To reach this level, sometimes two different time and spatial discretizations must have been used for the two solutes.

3 Results and discussion

Basic and surface properties

The seam material shows a neutral soil reaction with an average pH of 7.1 (SD = 0.2, N = 17). That is typical for urban soils. It is most likely caused by concrete abrasions from buildings or salts (Burghardt, 1994). For the seam material, additionally the adja-

Filter properties of pavement seam materials

T. Nehls et al.

Title Page

Abstract

Introduction

Conclusions

References

Tables

Figures

◀

▶

◀

▶

Back

Close

Full Screen / Esc

Printer-friendly Version

Interactive Discussion

cent pavers can be direct sources of constant carbonate intake as pedestrians not only abrade the soles of their shoes but also the surface of concrete or limestone pavers. The difference of C_{tot} and C_{org} , most probably carbonates, is 5 g kg^{-1} ($SD = 2 \text{ g kg}^{-1}$, $N = 18$). The slightly higher pH of the Warsaw samples may be due to salinity effects.

At least the EC is significantly higher in Warsaw compared to Berlin ($p < 0.05$, $N = 20$) (Table 2). The reason for the higher ECs is a more frequently use of deicing salts on streets of Warsaw compared to Berlin. There was no difference between the seam material and the original construction sand detectable. However, from the point of view of the high pH a pronounced HM displacement must not be suspected.

The seam material is dark. The Munsell colors objectively prove and quantify this observation (Table 2). Like in “natural” soils this coloration can be explained by an enrichment of organic matter, which in this case could be black soot (Nehls et al., 2007¹). Measured C_{org} varies from 12 to 48 g kg^{-1} in the 0 to 1 cm layer and is higher than in the 1 to 5 cm layer (less than 3 g kg^{-1}) (Table 2). A displacement of C_{org} into the 1 to 5 cm layer cannot be excluded, but must be expected (Fig. 2). However, the low C_{org} contents in the deeper layer allows to regard the 1 to 5 cm layer as original and not altered. Besides that, it cannot be excluded, that the construction sand already contained different amounts and forms of organic matter.

The CEC_{pot} of the 0 to 1 cm layer in Berlin is not significantly different from that in Warsaw. With 1.2 to $4.8 \text{ cmol}(+) \text{ kg}^{-1}$ the CEC_{pot} of the seam material is low compared to values of 12 to $20 \text{ cmol}(+) \text{ kg}^{-1}$ for non-urban German sandy soils (Renger, 1965) or compared to values of 8 to $36 \text{ cmol}(+) \text{ kg}^{-1}$ for Berlin sandy forest soils with similar C_{org} contents (Wilczynski et al., 1993).

With $0.5 \text{ cmol}(+) \text{ kg}^{-1}$ soil, the CEC_{pot} of the 1 to 5 cm layer is significantly smaller than in the first layer. Compared to the original seam filling represented by the 1 to 5 cm layer, the depositions of urban dirt lead to an approximately four times higher CEC_{pot} in the seam material. Like for other sandy soils (Renger, 1965) the CEC of the seam material depends mainly on organic material. The CEC_{pot} of seam materials is propor-

tional to A_s which depends on C_{org} (Figs. 5 and 6) and both regression lines intersect the y-axis close to (0;0), which indicates that only C_{org} compounds contribute substantially to A_s and after all to CEC_{pot} .

Due to its special quality, the contribution of the seam material's C_{org} to CEC_{pot} is only $74 \text{ cmol}(+) \text{ kg}^{-1} \text{ C}$, (Fig. 5). However, the CEC of common, more natural soil organic matter has been estimated to be around $300 \text{ cmol}(+) \text{ kg}^{-1} \text{ C}$ by Parfitt et al. (1995) for New Zealand soils and by Krogh et al. (2000) for Danish soils. Higher values of up to $680 \text{ cmol}(+) \text{ kg}^{-1} \text{ C}$ were observed in acidic sandy forest soils (Wilczynski et al., 1993).

As mentioned above, the organic matter consists of different constituents, not everything can be referred to as humus. Combustion residues (BC) for instance account for up to one third of the C_{org} fraction (Nehls et al., 2007¹). Although they contribute to the CEC of soils, its contribution is lower than that of humus (Tryon, 1948). Consequently, the CEC_{pot} of the OM rises, if not C_{org} but $(C_{org} - BC)$ is applied for the correlation ($83 \text{ cmol}(+) \text{ kg}^{-1} \text{ C}$ ($r^2=0.74$) for C_{org} and $93 \text{ cmol}(+) \text{ kg}^{-1} \text{ C}$ ($r^2=0.74$) if $C=C_{org}-BC$ is applied).

The low contribution of C_{org} to CEC_{pot} can be explained by its low specific surface area (Fig. 6) and its low surface charge density. The first of the two reasons can be ascribed to the spheroidal particular character of the C_{org} (Nehls et al., 2006) resulting in low surface areas per weight (presuming similar substance densities) compared to humus. The samples from Berlin and Warsaw show a very similar behavior resulting in a good correlation between C_{org} and specific surface area ($r^2 = 0.8$). As it can be seen from the slope of the linear regression line, the specific surface area of the seam material's C_{org} is about $516 \text{ m}^2 \text{ g}^{-1}$. Wilczynski et al. (1993) investigated a Berlin forest soil using the same methodology for measuring specific surface areas. They found the contribution of C_{org} to A_s to be up to $1062 \text{ m}^2 \text{ g}^{-1}$.

The SCD of a soil sample is a measure for the quantity of polar functional groups. The SCD of the seam material is seven times lower than that of sandy forest soils (Wilczynski et al., 1993; Hajnos et al., 2003), which causes the comparable low

Filter properties of pavement seam materials

T. Nehls et al.

Title Page

Abstract

Introduction

Conclusions

References

Tables

Figures

◀

▶

◀

▶

Back

Close

Full Screen / Esc

Printer-friendly Version

Interactive Discussion

CEC at similar C_{org} levels (Fig. 5. Hajnos et al. (2003) report on SCD of 2.9 to $10.6 \times 10^{-6} \text{ mol}(+) \text{ m}^{-2}$ for Berlin sandy forest soils, while the SCD of seam material is not greater than $1.2 \times 10^{-6} \text{ mol}(+) \text{ m}^{-2}$. The low SCD of the seam material's C_{org} is caused by unpolar organic substances.

This statement is supported by the investigated distribution of adsorption energies (Fig. 7). Medium energy sites dominate in the original construction sand. In the studied seam materials the water binding forces are lower. Most of the seam materials show a high number of low energy sites and only a low number of higher energy sites. This indicates a higher fraction of polar surfaces in the lower layer. The shift between the construction sand and the seam material is caused by the accumulation of non-polar substances, mainly organic material. Additionally to the accumulation, organic substances may have coated the polar mineral surfaces in the upper layer.

Higher polarity usually results in higher SCD. However, there is no dependence between E_a and SCD for the seam material. Possibly, it has been shadowed by the salt accumulation effects, because E_a was found to be related to the EC of the studied seam materials. The E_a decreases with an increase of EC which is connected logarithmically with low hydration energy of the salt cations. Similar relations of adsorption energy and parameters related to soil salinity are observed in natural saline environments (Toth and Jozefaciuk, 2002).

The investigation of SCD and E_a revealed characteristics of the seam materials OM, which should be validated by analysis of the quality and quantity of functional groups, e.g. using solid phase ^{13}C nuclear magnetic resonance spectroscopy (Preston, 1996; Baldock et al., 1992) or FT-IR spectroscopy (Ellerbrock et al., 1999).

Heavy metal adsorption

The variations for the Freundlich parameters as well as for the background contaminations are high, especially regarding comparable pH values. The Freundlich K_f values for Pb and Cd are higher in the 0 to 1 cm layer than in the 1 to 5 cm layer. The values

Filter properties of pavement seam materials

T. Nehls et al.

Title Page

Abstract

Introduction

Conclusions

References

Tables

Figures

◀

▶

◀

▶

Back

Close

Full Screen / Esc

Printer-friendly Version

Interactive Discussion

for m are similar for both depths. However, a comparison of K_f without considering m is not meaningful. Therefore, the retardation factors were calculated, which consider both parameters. They vary from 2056 to around 95 000 for Pb and from 26 to 608 for Cd for the described case (Table 3). Thereby, the comparison between the seam material and the original seam filling reveals a clear positive effect of the depositions in the seam material.

Pb adsorption

For samples from Berlin, the higher adsorption potential of the seam material compared to the construction sand corresponds to higher C_{org} contents, which is expressed by the correlation of the retardation factor, R and C_{org} [$g\ g^{-1}$] ($R = 281986 C_{org} + 3600$; $r^2 = 0.82$). Thereby, two samples have been excluded from the dataset: B1 and B2. For both samples, the Freundlich parameters were fitted with a specified range for m : $0 \leq m \leq 1$ to meet the conditions for Freundlich's model stated by Sposito (1980). However, in all investigated parameters they behave not different from the other samples, except for the total concentrations of Pb, which are comparably low.

There is no correlation of C_{org} and R for the Warsaw samples ($R = 10^6 C_{org} + 9920$, $r^2 = 0.15$). If the sample W1 is excluded from the dataset for the same reasons like B1 and B2, the correlation is more significant but the resulting regression function makes no sense ($R = 2 \times 10^6 C_{org} - 4243$, $r^2 = 0.64$). However, the samples from Warsaw have higher R ($p < 0.05$, $N = 9$) at similar C_{org} , caused by higher K_f ($p < 0.05$, $N = 9$) and similar values for m . Following Sposito (1980) that indicates a higher variance of adsorbers in Warsaw, providing adsorption sites with a broader range of Pb adsorption energies. This might be due to, (i) a different kind of organic matter in Warsaw, which provides more adsorption sites for Pb compared to Berlin. However, this is not supported by different water adsorption energies (E_a) nor by different surface areas or different Pb amounts whether total or EDTA extractable amounts. More likely, it shows (ii) the greater importance of other adsorbers than the studied organic substances for

Filter properties of pavement seam materials

T. Nehls et al.

Title Page

Abstract

Introduction

Conclusions

References

Tables

Figures

◀

▶

◀

▶

Back

Close

Full Screen / Esc

Printer-friendly Version

Interactive Discussion

the Warsaw samples. In Berlin, Pb_{tot} correlates very well with C_{org} , indicating same sources, e.g. combustion processes and/or strong adsorption of Pb on organic matter. However, the lacking correlation for the Warsaw samples could also be an effect of (iii) the small number of samples compared to the high spatial variability in urban soils.

5 Cd adsorption

The adsorption of Cd to the soil substrate is higher in the seam material compared to the original construction material. All retardation factors are higher for the seam material compared to the construction sand (Table 3). Compared to Pb, for Cd the improved sorption capacity is not a result of the deposition of organic material, as there is no correlation between R and C_{org} , nor Cd_{tot} and C_{org} . So the deposition of other adsorbers, which have not been studied here, must be relevant. However, there is also no difference in the adsorption behaviour of samples from Warsaw or Berlin towards Cd.

Compared to natural sandy soils, the seam material shows a similar retardation towards Pb but a very low retardation of Cd. Kocher (2005) investigated sandy soils along federal highways in Germany for their HM retention while Adhikari and Singh (2003) investigated sandy soils from India and England (Table 4). The soils A1, A2, and A3 had higher C_{org} (31, 50, and 50 g kg^{-1}) and slightly lower pH values (6.5, 6.6, and 6.1) but were comparable in terms of clay content. For a comparison, the retardation factors were computed for the same case like in table 3. For Pb, the values are slightly, but not significantly higher. This is due to similar K_f , but very low values for m (0.24, 0.18, and 0.08) indicating a highly non-linear adsorption favouring adsorption at low concentrations.

For Cd Kocher (2005) reports of very similar m values, while the values for K_f are significantly higher in road side soils compared to seam materials. So, the Cd retardation in roadside soils is clearly higher compared to seam materials.

Filter properties of pavement seam materials

T. Nehls et al.

Title Page

Abstract

Introduction

Conclusions

References

Tables

Figures

◀

▶

◀

▶

Back

Close

Full Screen / Esc

Printer-friendly Version

Interactive Discussion

Simulated HM displacement

For the groundwater recharge rate of 120 mm a^{-1} , the simulated displacement times vary from 315 to 2350 a for Pb and from 37 to 253 a for Cd (Table 5). At the site B2, the measured Pb concentration for the liquid phase in the soil is already higher than the concentration in the rainwater runoff. For Cd, however all sites show higher soil water than rainwater concentrations. In these scenarios, every rainfall is a net HM displacement! Apart from these cases, the positive filter effects of urban depositions, which were already discussed by means of retardation factors, could be approved by the simulations for all cases but one. In the simulations, besides adsorption behaviour, also the soil hydraulic properties and densities were considered. The effect of the smaller dry bulk density of the seam material can compensate the effect of stronger adsorption. The displacement of Cd at the site B4 is the one example. If the scenarios *ia* and *iiia* for the site B4 are calculated with the original seam filling's dry bulk densities, the travel time through the seam material would be 105 a and therefore higher than that of the original seam filling. So except for the displacement of Cd at the site B4 we conclude that in general, the seam material has a positive impact on the retardation of Cd and Pb. Although the impact is detectable, it is not very high and the formation of only 1 cm thick layer of seam material leads not to substantial longer travel times. However, the potential of the urban dirt as a Pb filter is clearly to be seen if the scenarios *iiib* are compared to scenarios *ia*: even contaminated seam material is a much better filter than any clean construction sand can be. For Cd, the background contamination is that high, that both seam material and original construction sand act rather as a source than as a sink. For Pb however, the calculated traveltimes do not imply an acute risk of groundwater contamination.

Because of the abundance of ponds at streets and sidewalks in urban areas, we simulated the infiltration of accumulated rainwater runoff from ponds. Realizing a higher infiltration rate of 0.48 instead of 0.12 cm d^{-1} influences the soil water content and therefore the pore water velocities. The average ratio between the traveltimes for

HESSD

4, 2625–2657, 2007

Filter properties of pavement seam materials

T. Nehls et al.

Title Page

Abstract

Introduction

Conclusions

References

Tables

Figures

◀

▶

◀

▶

Back

Close

Full Screen / Esc

Printer-friendly Version

Interactive Discussion

EGU

120 mm a⁻¹ and 480 mm a⁻¹ is 1/4. The calculated travel times range from 10 to 100 a for Cd. As the pavements at the investigated sites were constructed from the early 1900s on, a substantial amount of heavy metals may already have left the upper soil layers. The displacement risk for Pb even from ponds is rather low. However, the simulated infiltration from ponds shows the high importance of non-uniform infiltration in urban areas. It therefore underlines the need of knowledge on soil surface properties for realistic risk assessments, e.g. for more mobile substances such as glyphosate (Kempenaar et al., 2007).

4 Conclusions

Depositions of all kinds of urban dirt form the seam material, which has different properties than the original material. Compared to the original construction sand, the depositions lead to increased specific surface area and cation exchange capacity. Compared to natural organic matter this anthropogenic form of organic material has a rather small surface area and surface charge density which results in comparable low cation exchange capacity.

In terms of heavy metal mobilisation and retention the seam material can act as a filter and a source depending on the element. Thereby the source as well as the filter-effect are low because of the typical thin layer of only 1 cm. However, the simulated break through times for one dimensional matrix flow suggest, that there is no general risk of a groundwater contamination from traffic released Cd and Pb. However, the infiltration of rainwater runoff from ponds can lead to fast displacement of Cd, which may leave the pavement system after only a decade. We conclude, that the seam material is an interesting model substrate to show the positive impacts of deposited dust on ecological soil functions.

Acknowledgements. We gratefully thank the DFG (WE 1125/18-1) and the Polish Academy of Sciences for funding. Furthermore, the author especially thanks H. Stoffregen for the discussions.

Filter properties of pavement seam materials

T. Nehls et al.

Title Page

Abstract

Introduction

Conclusions

References

Tables

Figures

◀

▶

◀

▶

Back

Close

Full Screen / Esc

Printer-friendly Version

Interactive Discussion

References

- Adhikari, T. and Singh, M.: Sorption characteristics of lead and cadmium in some soils of India, *Geoderma*, 114, 81–92, 2003. [2640](#), [2649](#)
- Aranovich, G.: The theory of polymolecular adsorption, *Langmuir*, 8, 736–739, 1992. [2630](#),
5 [2631](#)
- Baldock, J. A., Oades, J. M., Waters, A. G., Peng, X., Vassallo, A. M., and Wilson, M. A.: Aspects of the Chemical-Structure of Soil Organic Materials as Revealed by Solid-State C-13 Nmr-Spectroscopy, *Biogeochemistry*, 16, 1–42, 1992. [2638](#)
- Boller, M.: Tracking heavy metals reveals sustainability deficits of urban drainage systems, *Wat.Sci.Tech.*, 35, 77–87, 1997. [2627](#)
10
- Brunauer, S., Emmett, P. H., and Teller, E.: Adsorption of gases in multimolecular layers, *Journal of the American Chemical Society*, 60, 309–319, 1938. [2630](#)
- Burghardt, W.: Soils in urban and industrial environments, *Journal of Plant Nutrition and Soil Science*, 157, 205–214, 1994. [2635](#)
- 15 Dannecker, W., Au, M., and Stechmann, H.: Substance Load in Rainwater Runoff from Different Streets in Hamburg, *The Science of the total environment*, 93, 385–392, 1990. [2627](#)
- Dierkes, C. and Geiger, W. F.: Pollution retention capabilities of roadside soils, *Water Science and Technology*, 39, 201–208, 1999. [2627](#)
- Ellerbrock, R., Hoehn, A., and Gerke, H.: Characterization of soil organic matter from a sandy
20 soil in relation to management practice using FT-IR, *Plant and Soil*, 213, 55–61, 1999. [2638](#)
- Hajnos, M., Jozefaciuk, G., Sokolowska, Z., Greiffenhagen, A., and Wessolek, G.: Water storage, surface, and structural properties of sandy forest humus horizons, *Journal of Plant Nutrition and Soil Science-Zeitschrift Fur Pflanzenernahrung Und Bodenkunde*, 166, 625–634, 2003. [2637](#), [2638](#)
- 25 Harris, L.: Adsorption on a patchwise heterogeneous surface. I. Mathematical analysis of the step function approximation of the local isotherm, *Surface Science*, 10, 129–145, 1968. [2631](#)
- Heinzmann, B.: Improvement of the surface water quality in the Berlin region, *Water Science and Technology*, 38, 191–200, 1998. [2626](#)
- Jaroniec, M. and Brauer, P.: Recent progress in determination of energetic heterogeneity of
30 solids from adsorption data, *Surface Science Reports*, 6, 65–117, 1986. [2631](#)
- Jozefaciuk, G. and Shin, J.: Water vapor adsorption on soils. II. Estimation of adsorption energy distributions using local BET and Aranovich isotherms, *Korean Journal of Soil Science and*

HESSD

4, 2625–2657, 2007

Filter properties of pavement seam materials

T. Nehls et al.

Title Page

Abstract

Introduction

Conclusions

References

Tables

Figures

◀

▶

◀

▶

Back

Close

Full Screen / Esc

Printer-friendly Version

Interactive Discussion

EGU

- Fertilizer, 29, 218–225, 1996. [2632](#)
- Kempenaar, C., Lotz, L. A. P., van der Horst, C. L. M., Beltman, W. H. J., Leemans, K. J. M., and Bannink, A. D.: Trade off between costs and environmental effects of weed control on pavements, *Crop Protection*, 26, 430–435, 2007. [2642](#)
- 5 Kocher, B.: Einträge und Verlagerung strassenverkehrsbedingter Schwermetalle in Sandböden an stark befahrenen Ausserortstrassen, Dissertation, Institut für Ökologie, Technische Universität Berlin, 2005. [2640](#), [2649](#)
- Krogh, L., Breuning-Madsen, H., and Greve, M. H.: Cation-exchange capacity pedotransfer functions for Danish soils, *Acta Agriculturae Scandinavica Section B-Soil and Plant Science*, 50, 1–12, 2000. [2637](#)
- 10 Mehlich, A.: Mehlich-3 soil test extractant: a modification of Mehlich-2 extractant, *Communications in soil science and plant analysis*, 15, 1409–1416, 1984. [2629](#)
- Nehls, T., Jozefaciuk, G., Sokolowska, Z., Hajnos, M., and Wessolek, G.: Pore-system characteristics of pavement seam materials of urban sites, *Journal of Plant Nutrition and Soil Science*, 169, 16–24, 2006. [2627](#), [2635](#), [2637](#)
- 15 Novakov, T.: The role of soot and primary oxidants in atmospheric chemistry, *The science of the total environment*, 36, 1–10, 1984. [2628](#)
- OECD: OECD GUIDELINE FOR THE TESTING OF CHEMICALS No. 106 Adsorption - Desorption Using a Batch Equilibrium Method, 2000. [2632](#)
- 20 Parfitt, R., Giltrap, D., and Whitton, J.: Contribution of organic matter and clay minerals to the cation exchange capacity of soils, *Communications in soil science and plant analysis*, 26, 1343–1355, 1995. [2637](#)
- Preston, C. M.: Applications of NMR to soil organic matter analysis: History and prospects, *Soil Science*, 161, 144–166, 1996. [2638](#)
- 25 Renger, M.: Berechnung der Austauschkapazität der organischen und anorganischen Anteile der Böden, *Zeitschrift für Pflanzenernährung und Bodenkunde*, 110, 10–26, 1965. [2636](#), [2655](#)
- Simunek, J., Sejna, M., and vanGenuchten, M.: The HYDRUS-2D Software Package for Simulating the two-dimensional movement of water, heat, and multiple solutes in variably-saturated media, Tech. rep., U.S. Salinity Laboratory, Riverside, CA 92507, 1999. [2634](#)
- 30 Sposito, G.: Derivation of the Freundlich Equation for Ion Exchange Reactions in Soils, *Soil Science Society of America Journal*, 44, 652–654, 1980. [2633](#), [2639](#)
- Stumm, W. and Morgan, J.: *Aquatic Chemistry*, John Wiley and Sons, Inc., New York, 3 rd ed.

**Filter properties of
pavement seam
materials**

T. Nehls et al.

Title Page

Abstract

Introduction

Conclusions

References

Tables

Figures

◀

▶

◀

▶

Back

Close

Full Screen / Esc

Printer-friendly Version

Interactive Discussion

edn., 1996. [2633](#)

Toth, T. and Jozefaciuk, G.: Physicochemical properties of a solonetzic toposequence, *Geoderma*, 106, 137–159, 2002. [2638](#)

Tryon, E.: Effect of Charcoal on certain physical, chemical and biological properties of forest soils, *Ecological Monographs*, 18, 82–114, 1948. [2637](#)

Welp, G. and Brummer, G. W.: Adsorption and solubility of ten metals in soil samples of different composition, *Journal of Plant Nutrition and Soil Science-Zeitschrift Fur Pflanzenernahrung Und Bodenkunde*, 162, 155–161, 1999. [2633](#)

Wessolek, G. and Facklam, M.: Standorteigenschaften und Wasserhaushalt von versiegelten Flächen, *Journal of Plant Nutrition and Soil Science*, 160, 41–46, 1997. [2627](#)

Wessolek, G. and Renger, M.: Bodenwasser- und Grundwasserhaushalt, in: *Stadtökologie*, edited by Sukopp, H. and Wittig, R., pp. 186–200, Gustav Fischer, Stuttgart, 1998. [2627](#), [2634](#)

Wilczynski, W., Renger, M., Jozefaciuk, G., Hajnos, M., and Sokolowska, Z.: Surface area and CEC as related to qualitative and quantitative changes of forest soil organic matter after liming, *Zeitschrift für Pflanzenernahrung und Bodenkunde*, 156, 235–238, 1993. [2636](#), [2637](#), [2655](#), [2656](#)

HESSD

4, 2625–2657, 2007

Filter properties of pavement seam materials

T. Nehls et al.

Title Page

Abstract

Introduction

Conclusions

References

Tables

Figures

◀

▶

◀

▶

Back

Close

Full Screen / Esc

Printer-friendly Version

Interactive Discussion

Filter properties of pavement seam materials

T. Nehls et al.

Table 1. Input parameters for the numerical simulation of heavy metal displacement through a pavement soil column. K_{S^*} and Θ_{S^*} indicate derived effective model parameters for realizing the water flow.

general model parameters								
length unit: cm, time unit: d, mass unit: mg length of the column: 20 cm; number of nodes: 101 upper boundary condition: constant pressure head Ψ_u lower boundary condition: constant pressure head Ψ_l								
seam material			construction sand					
soil hydraulic parameters								
Θ_r [cm ³ cm ⁻³]	0.117			0.058				
Θ_s [cm ³ cm ⁻³]	0.527			0.424				
α [cm ⁻¹]	0.034			0.058				
\bar{n} [-]	1.514			1.401				
K_S [cm d ⁻¹]	715			374				
ρ_B [g cm ⁻³]	1.16			1.51				
water flow parameters in the model								
$\Psi_u = \Psi_l$ [cm]	0							
$K_{S^*1,2}$ [cm d ⁻¹]	0.12, 0.48							
Θ_{S^*} [cm ³ cm ⁻³]	0.264 for K_{S^*1} (0.298 for K_{S^*2})				0.231 for K_{S^*1} (0.265 for K_{S^*2})			
adsorption parameters								
	B1	B2	B4	B9	B1a	B2a	B4a	B9a
$K_f(\text{Pb})$ [mg ^{1-m} L ^m kg ⁻¹]	2638	2133	1321	1416	499	272	833	738
$m(\text{Pb})$ [-]	1.00	1.00	0.45	0.62	0.92	1.00	0.55	0.62
$c_{\text{Pb}}(\text{soil water})$ [mg L ⁻¹]	0	0.22	0.02	0.04	0.04	0.46	0.01	0.01
$c_{\text{Pb}}(\text{rainwater})$ [mg L ⁻¹]	0.3							
$K_f(\text{Cd})$ [mg ^{1-m} L ^m kg ⁻¹]	20.38	16.95	19.37	15.18	6.92	5.41	5.66	8.61
$m(\text{Cd})$ [-]	0.70	0.38	0.62	0.28	0.63	0.41	0.40	0.34
$c_{\text{Cd}}(\text{soil water})$ [mg L ⁻¹]	0.013	0.020	0.004	0.020	0.023	0.013	0.020	0.019
$c_{\text{Cd}}(\text{rainwater})$ [mg L ⁻¹]	0.01							

Title Page

Abstract

Introduction

Conclusions

References

Tables

Figures

◀

▶

◀

▶

Back

Close

Full Screen / Esc

Printer-friendly Version

Interactive Discussion

Table 2. Surface properties and general characteristics of seam materials and original seam fillings from Berlin and Warsaw. Values in one column followed by the same letter are not significantly different at $p < 0.05$; $N = 20$.

Site	Munsell Color	pH (CaCl ₂)	EC 10 ⁻⁶ S cm ⁻¹	CEC _{pot} cmol(+) kg ⁻¹	C _{tot} g kg ⁻¹	C _{org} g kg ⁻¹	A _s (H ₂ O) m ² g ⁻¹	SCD μmol(+) m ⁻²	\bar{E}_a
Berlin, 0 to 1 cm									
B1	2.5Y3/2	6.84	107 b	1.78	19.20	14.33	14.81	1.20	3.08
B2	2.5Y3/2	7.07	93 b	1.65	18.70	16.23	12.44	1.32	3.22
B3	2.5Y2.5/1	7.11	-	1.96	33.37	27.60	17.00	1.15	2.82
B4	2.5Y3/1	7.22	143 b	1.98	25.49	23.16	12.17	1.62	3.30
B5	2.5Y3/1	7.28	161 b	1.86	23.01	21.80	13.56	1.37	3.06
B6	2.5Y3/1	6.80	76 b	1.23	17.55	12.01	8.87	1.39	3.41
B7	2.5Y3/1	7.21	87 b	1.21	21.00	18.60	12.69	0.95	3.06
B8	2.5Y3/1	7.08	101 b	1.29	15.81	13.06	11.03	1.17	3.22
B9	10YR2/1	7.05	79 b	1.82	22.92	18.40	14.03	1.30	3.04
B10	10YR2/1	6.58	114 b	4.78	52.69	48.20	29.25	1.64	2.82
Berlin, 1 to 5 cm									
B1a	10YR4/6	7.12	48 c	0.76	5.11	3.80	7.46	1.02	3.41
B2a	10YR5/6	7.03	21 c	0.18	1.78	1.67	5.30	0.34	3.86
B3a	2.5Y4/3	7.05	-	-	4.42	3.08	5.20	n.d.	3.88
B4a	2.5Y5/3	7.13	28 c	0.43	2.24	1.69	3.00	1.44	4.32
Warsaw, 0 to 1 cm									
W1	2.5Y2.5/1	-	306 a	2.14	29.47	22.84	13.82	1.55	
W2	2.5Y2.5/1	6.91	402 a	1.89	43.40	35.37	20.41	0.93	3.10
W3	2.5Y2.5/1	7.35	328 a	3.36	32.30	27.90	27.76	1.21	2.91
W4	2.5Y3/1	7.41	409 a	1.69	26.86	20.80	12.80	1.32	2.79
W5	10YR2/1	7.29	426 a	2.06	35.58	27.93	17.76	1.16	2.71
W6	2.5Y3/1	7.34	440 a	1.50	32.32	25.70	15.85	0.94	2.90
W8	2.5Y3/1	7.23	2040 a	0.70	18.74	12.40	11.32	0.61	2.64
W9	2.5Y3/2	7.36	1927 a	1.20	21.80	15.56	14.85	0.80	1.27

Filter properties of pavement seam materials

T. Nehls et al.

Title Page

Abstract Introduction

Conclusions References

Tables Figures

◀ ▶

◀ ▶

Back Close

Full Screen / Esc

Printer-friendly Version

Interactive Discussion

Table 3. Heavy metal adsorption parameters of seam material from Berlin and Warsaw.

Site	$K_f(\text{Pb})$ $\text{mg}^{1-m} \text{L}^m \text{kg}^{-1}$	$m\text{Pb}$	r^2	Pb_{tot} mg kg^{-1}	$R_{\text{Pb}}^{(a)}$	$K_f(\text{Cd})$ $\text{mg}^{1-m} \text{L}^m \text{kg}^{-1}$	$m\text{Cd}$	r^2	Cd_{tot} mg kg^{-1}	$R_{\text{Cd}}^{(a)}$
Berlin, 0 to 1 cm										
B1	2638 ^(b)	1.00	0.87	68.5	19919	20.4	0.70	0.98	2.0	147
B2	2133 ^(b)	1.00	0.71	91.0	15916	17.0	0.38	0.99	9.5	155
B4	1321	0.45	0.93	309.5	8685	19.4	0.62	0.99	n.d.	162
B5	977	0.44	0.96	290.2	6398	12.2	0.54	0.94	2.0	108
B6	1111	0.54	0.84	190.1	7901	12.2	0.21	0.93	6.1	82
B7	1376	0.93	0.96	222.0	10518	13.0	0.25	0.96	8.4	100
B8	1056	0.58	0.91	163.4	7653	16.5	0.29	0.98	6.9	121
B9	1416	0.62	0.86	203.5	10476	14.2	0.48	0.94	2.0	119
B10	2483	0.57	0.95	480.0	17914	15.2	0.28	0.98	6.1	110
Berlin, 1 to 5 cm										
B1a	499	0.92	0.96	38.3	3817	6.9	0.63	0.81	2.1	62
B2a	272 ^(b)	1.00	0.99	49.6	2056	5.4	0.41	0.99	5.2	53
B4a	833	0.55	0.95	72.6	5961	5.7	0.40	0.69	4.0	43
B9a	738	0.62	0.93	135.6	5449	8.6	0.34	0.99	13.0	82
Warsaw, 0 to 1 cm										
W1	12558 ^(b)	1.00	0.97	148.1	94817	20.3	0.30	0.98	2.9	145
W2	8052	0.89	0.97	180.9	61784	11.9	0.18	0.85	5.1	87
W3	4699	0.76	0.95	159.3	35982	12.1	0.15	0.76	5.5	77
W5	2738	0.91	0.87	99.7	20965	33.6	0.28	0.90	8.5	280
W8	2234	0.75	0.98	98.5	17088	8.4	0.10	0.89	5.2	42
W9	3078	0.88	0.89	270.7	23627	79.2	0.55	0.99	5.0	485

^(a) $\rho_B = 1.5 \text{ g cm}^{-3}$, $C_f = 0.1 \text{ mg L}^{-1}$, $\Theta = 0.3 \text{ m}^3 \text{ m}^{-3}$

^(b) isotherms were fitted with $0 \leq m \leq 1$

Filter properties of pavement seam materials

T. Nehls et al.

Title Page

Abstract

Introduction

Conclusions

References

Tables

Figures

◀

▶

◀

▶

Back

Close

Full Screen / Esc

Printer-friendly Version

Interactive Discussion

Filter properties of pavement seam materials

T. Nehls et al.

Table 4. Published adsorption data for soils comparable to seam material concerning organic matter and clay content.

soil	Pb			Cd		
	K_f $\text{dm}^3 \text{kg}^{-1}$	m -	$R^{(a)}$ -	K_f $\text{dm}^3 \text{kg}^{-1}$	m -	R^* -
Kocher (2005)						
jAh,0 to 10 cm,A1,1m	6849	0.24	47118	120	0.50	949
jAh,0 to 25 cm,A2,1m	8495	0.18	50017	101	0.50	800
jAh,0 to 18 cm,A3,1m	43720	0.08	143973	97	0.55	751
Adhikari and Singh (2003)						
Eng2, Norfolk	2239	0.73	15188	316	0.92	1752
Ind2, Ganges plains	102094	0.73	693895	1409	0.80	8973
Ind5, Desert sand	1135	0.42	9065	76	0.62	564

^(a) $\rho_B=1.5 \text{ g cm}^{-3}$, $C_f=0.1 \text{ mg L}^{-1}$, $\Theta=0.3 \text{ m}^3 \text{ m}^{-3}$

Title Page

Abstract Introduction

Conclusions References

Tables Figures

◀ ▶

◀ ▶

Back Close

Full Screen / Esc

Printer-friendly Version

Interactive Discussion

Filter properties of pavement seam materials

T. Nehls et al.

Table 5. Simulated heavy metal displacement through a 20 cm paved soil column at different sites in Berlin. ^a The travel times indicate the period which is needed to recover 95 % of the applied concentration at the lower boundary of the soil column.

Scenario	Pb				Cd			
	B1	B2	B4	B9	B1	B2	B4	B9
	travel time ^a [a] for 120 mm a ⁻¹							
ia (uncontaminated sand)	610	315	1253	1072	37	92	100.8	176
ib (contaminated sand)	584	0	1159	1016	0	0	0	0
ii (uncontaminated sand with seam material)	612	320	1255	1075	39	93	101.4	179
iiia (contaminated sand with seam material)	588	0	1158	1008	0	0	0	0
iiia (uncontaminated seam material)	2350	1901	1603	1578	90	185	83	253
iiib (contaminated seam material)	2350	1315	1341	1392	0	0	60	0

Title Page

Abstract

Introduction

Conclusions

References

Tables

Figures

◀

▶

◀

▶

Back

Close

Full Screen / Esc

Printer-friendly Version

Interactive Discussion

Filter properties of pavement seam materials

T. Nehls et al.

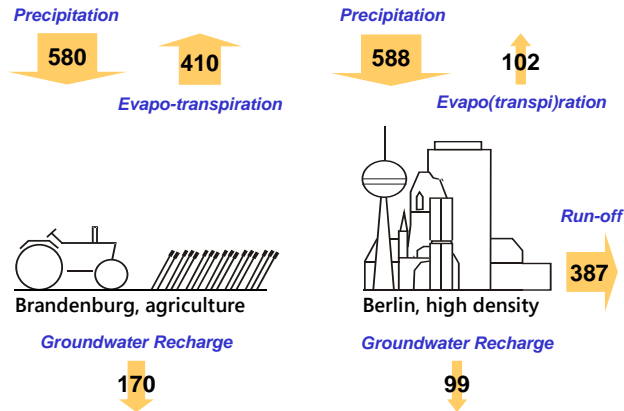


Fig. 1. Illustration of long term water balances for **(a)** an agricultural site outside Berlin and **(b)** a site with 85 to 100% surface sealing inside the city. The water balance components are given in mm a^{-1} .

Title Page	
Abstract	Introduction
Conclusions	References
Tables	Figures
◀	▶
◀	▶
Back	Close
Full Screen / Esc	
Printer-friendly Version	
Interactive Discussion	

Filter properties of pavement seam materials

T. Nehls et al.



Fig. 2. Dark seam material (0 to 1 cm) compared to the lighter original sandy seam filling (1 to 5 cm) at Weidendamm, Berlin.

Title Page

Abstract

Introduction

Conclusions

References

Tables

Figures

◀

▶

◀

▶

Back

Close

Full Screen / Esc

Printer-friendly Version

Interactive Discussion

Filter properties of pavement seam materials

T. Nehls et al.

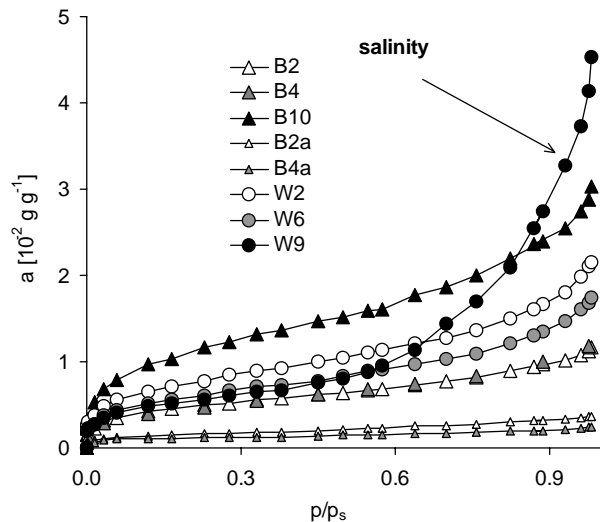


Fig. 3. Measured water-vapor adsorption isotherms for seam material of pavements in Berlin (B) and Warsaw (W); (a = amount of adsorbed water, p/p_s = water vapour pressure).

Title Page

Abstract

Introduction

Conclusions

References

Tables

Figures

◀

▶

◀

▶

Back

Close

Full Screen / Esc

Printer-friendly Version

Interactive Discussion



Fig. 4. Undisturbed sampling of seam material (0 to 1 cm) from a cobbled stone paved street using special 3.3 cm³ cylinders in an old residential area at the site Pfluegerstrasse, Berlin.

Filter properties of pavement seam materials

T. Nehls et al.

Title Page

Abstract

Introduction

Conclusions

References

Tables

Figures

◀

▶

◀

▶

Back

Close

Full Screen / Esc

Printer-friendly Version

Interactive Discussion

Filter properties of pavement seam materials

T. Nehls et al.

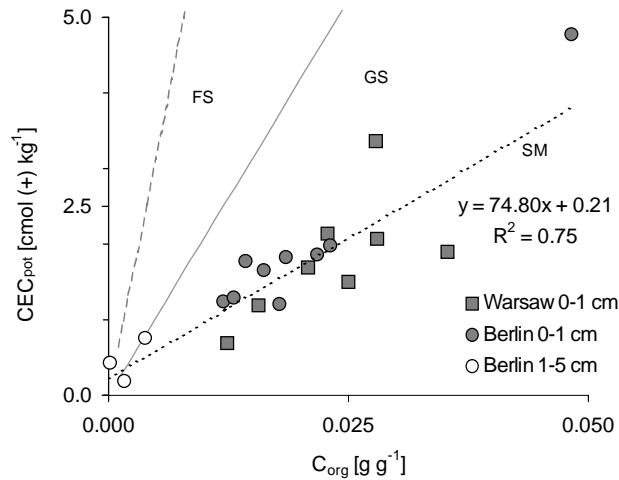


Fig. 5. CEC_{pot} depending on C_{org} in seam materials (SM, dotted), sandy German soils (GS, solid) (Renger, 1965) and sandy forest soils (FS, dashed) (Wilczynski et al., 1993).

Title Page

Abstract Introduction

Conclusions References

Tables Figures

◀ ▶

◀ ▶

Back Close

Full Screen / Esc

Printer-friendly Version

Interactive Discussion

Filter properties of pavement seam materials

T. Nehls et al.

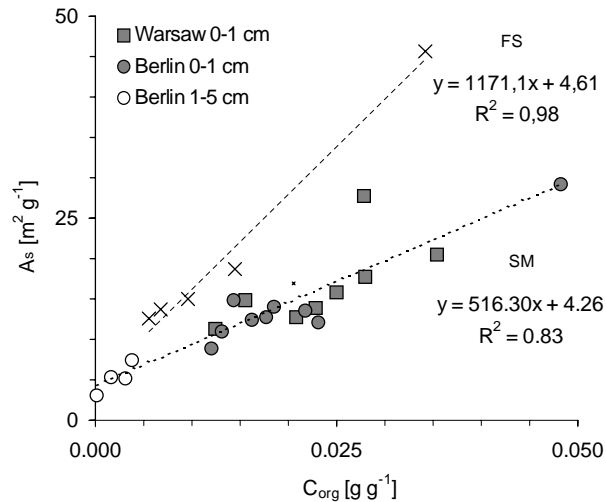


Fig. 6. Contribution of seam material's C_{org} (SM) to specific surface area measured by water vapour desorption isothermes A_s compared to forest soil's C_{org} (FS) investigated by Wilczynski et al. (1993).

Title Page

Abstract

Introduction

Conclusions

References

Tables

Figures

◀

▶

◀

▶

Back

Close

Full Screen / Esc

Printer-friendly Version

Interactive Discussion

Filter properties of pavement seam materials

T. Nehls et al.

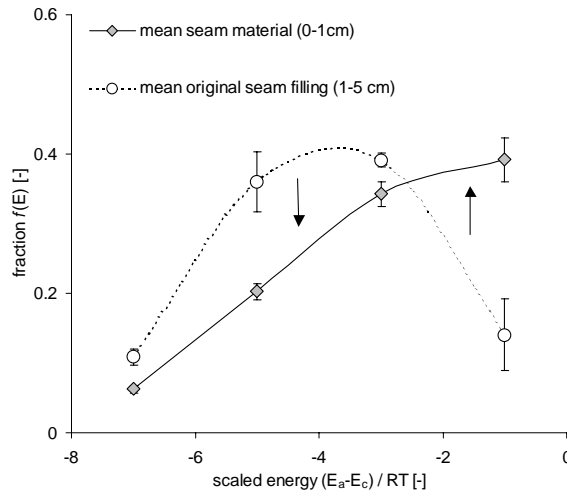


Fig. 7. Distribution of scaled adsorption energy levels for seam materials and original seam filling (sand) from Berlin and Warsaw. The arrows indicate the shift in adsorption energy fractions due to the deposition of urban dust. Error bars show standard errors, N = 19 for seam materials, N = 4 for original seam filling.

Title Page

Abstract

Introduction

Conclusions

References

Tables

Figures

◀

▶

◀

▶

Back

Close

Full Screen / Esc

Printer-friendly Version

Interactive Discussion